ELSEVIER

Applied Surface Science 182 (2001) 186–191

applied surface science

www.elsevier.com/locate/apsusc

Use of coherent X-ray diffraction to map strain fields in nanocrystals

I.K. Robinson*, I.A. Vartanyants

Loomis Laboratory of Physics, Department of Physics, University of Illinois, 1110 West Green Street, Urbana, IL 61801, USA

Abstract

A new method is proposed to analyze the internal strains inside nanometer-sized crystals. The method employs a coherent beam of X-rays to obtain a continuous diffraction pattern in the immediate vicinity of each of the Bragg reflections. The symmetric part of the diffraction is given by the Fourier transform of the crystal's shape, while the asymmetric part can be associated with the strain. Iterative Fourier transform methods can then be applied to reveal the strain as a three-dimensional spatial image.

Keywords: Nanocrystals; Internal strains; Iterative Fourier transform methods

1. Introduction

Coherent X-ray diffraction (CXD) occurs whenever the sample under investigation is smaller than the coherence of the X-ray beam used to measure it. With the availability of the new third generation synchrotron radiation sources, such as the European Synchrotron Radiation Facility (ESRF) and the Advanced Photon Source (APS), coherence lengths in the range of 10 μm (transverse) and 1 μm (longitudinal) are now available with sufficient flux to make such experiments practical. For the first time, we can now contemplate the situation in which the *entire sample lies within the coherence volume*, yet still obtain a measurable diffraction signal. This paper describes a potentially important application of CXD to measure the spatial distribution of the strain within a nanometer-sized crystal.

If a coherent beam is used to illuminate a small nanocrystal, for example in the 100 nm size range, its *complete* diffraction pattern can be measured using a typical direct-reading charge-coupled device (CCD) area detector, placed a few meters from the sample [1]. The coherence is required so that the diffraction from all the points in space within the crystal can interfere. The pattern is 'complete' in the sense that it is a perfectly resolved, continuous function of the reciprocal space. Instead of the customary ''finite-size'' broadening of the Bragg peaks [2], a detailed diffraction pattern results, with flares in the directions perpendicular to each of the crystal's facets. The existence of these flares was predicted by von Laue [3] and given the name ''Stacheln''. They have been observed routinely in studies of surface X-ray diffraction in the form of crystal truncation rods [4].

Fig. 1 shows the diffraction pattern expected from a small polyhedral crystal, obtained by Fourier transformation of its shape function. Perfect coherence was assumed. It is interesting to see not only the flares discussed above, but interference fringes as well. The

* Corresponding author. Tel.: +1-217-2442949; fax: +1-217-3336126.
E-mail address: ikr@uiuc.edu (I.K. Robinson).

0169-4332/01/$ – see front matter
PII: S0169-4332(01)00438-X

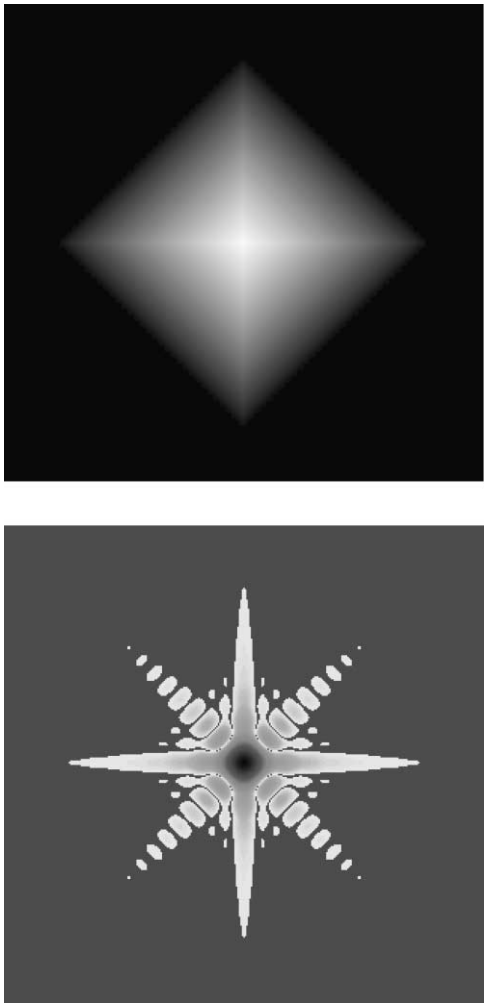

Fig. 1. Simulated diffraction pattern of the octohedral crystal shown in the upper panel. The 3D shape is projected onto the plane of the page, Fourier transformed in 2D and plotted as a contour map in the lower panel. This pattern is repeated around every reciprocal lattice point of the crystal's diffraction pattern.

flares become modulated into fringes when two faces of the crystal shape happen to be parallel. The example of Fig. 1 is in fact a very easy calculation to perform, accounting for *imperfect* coherence is considerably harder [5,6], but is essential in order to simulate the diffraction from any real distributions of objects. Patterns similar to that of Fig. 1 have been observed experimentally, as our group has demonstrated recently [1]. The patterns can be recorded fully in three dimensions (3D) as a set of 2D sections corresponding to the different angles on the rocking curve. Further discussion of the experiments can be found in ref. [1], here we will discuss the extension of the method to the imaging of strain fields inside the nanocrystals.

Because the pattern is a continuous function of reciprocal space, it can be sampled arbitrarily frequently with a suitable detector. Specifically, it can be sampled more often than the spatial Nyquist frequency, so that the inversion problem becomes mathematically overdetermined. ''Oversampling'' was proposed by Sayre [7] as a potential general method of solving the ''phase problem'' associated with inverting a diffraction pattern, at least in principle. Traditional crystallographic data are sampled at just one-half the spatial Nyquist frequency, so are not invertible directly. Oversampling can therefore be thought of being embodied in the crystallographic methods that exploit the non-crystallographic symmetry [8] or ''solvent flattening'' [9]. In these methods, sufficient redundancy exists in real space to reach the oversampled condition. A continuous diffraction pattern, on the other hand, can be oversampled directly in reciprocal space. This is the situation we consider in this paper.

Recently, Miao et al. have used oversampling to invert the forward scattering pattern of an artificial object measured with the soft X-rays [10]. Our group has demonstrated inversion of the hard X-ray diffraction data, measured around the (1 1 1) Bragg peak of a Au nanocrystal in the way described above, the result is a real-space density map which corresponds to the projection of the shape of the sample grain onto a plane [1]. The inversion works in two dimensions, and it is expected to work in three dimensions also.

For the reasons elaborated by Sayre [7], a more than two-fold over-sampled diffraction pattern is mathematically invertible *in principle*, it is not immediately clear that what computational methods would be efficient, considering that many thousands of equations must be solved. Crowther [11] has proposed a method to obtain the solution of the related problem of internal ''non-crystallographic'' symmetry, first discussed by Rossmann and Blow [12]. In the completely different context of spatial imaging, Gerchberg and Saxton (GS) [13] proposed more-or-less the same solution. The connection between the crystallographic and imaging problems was first noticed by Millane [14].

The GS method iterates back and forth between the real-space and reciprocal-space arrays, by means of discrete Fourier transforms, usually fast Fourier transforms (FFTs). The data array must be updated in both the spaces, to avoid simply backtracking. In reciprocal space, the data array is updated by asserting the measured amplitudes, while retaining the unmeasured phases, in real space, a variety of constraints can be employed to steer the solution towards the one that is consistent with the other knowledge of the system. In our case of finding the shape of a nanocrystal, the two real-space constraints are (i) it is real and (ii) it has ''finite support'', meaning that the crystal can only exist within a certain region of space. The size of this constraint region, which should be larger than the eventual crystal, can be estimated directly from the fringe spacing of the observed diffraction pattern. We demonstrated the utility of the GS method in the 1D case of CXD from silicon surfaces [15,16], and also in the 2D case of CXD from Au nanocrystals [1], where it was used in alternation with a related ''hybrid input–output'' computational method [17].

In the previous work, and in the discussion above, a nanocrystal is assumed to be made of atoms on a perfect space lattice, cut off by some boundary which defines its shape. Such a construction can be considered to be a multiplication of two functions, an infinite lattice of points and a binary-valued envelope. The diffraction pattern can then be constructed as the convolution of the Fourier transforms of these functions: the infinite lattice gives the reciprocal lattice, while the envelope (i.e. crystal shape) gives a general diffraction pattern that is localized near the origin, which it surrounds. This diffraction pattern has the usual centrosymmetry about the origin. When the convolution is evaluated, this diffraction pattern is copied to surround every point of the reciprocal lattice, making a periodic function. In this way, there is a *local* inversion symmetry about each reciprocal lattice point. This symmetry can be readily seen in Fig. 1, and is roughly what was observed in the experiments on gold nanocrystals [1].

When the crystal is strained, its atoms no longer lie on ideal lattice points, but are displaced slightly. This breaks the symmetry of the diffraction in the way, that is illustrated in Fig. 2. The upper panel of this 1D example shows a finite array of equally spaced atoms and its familiar diffraction pattern. The pattern is both

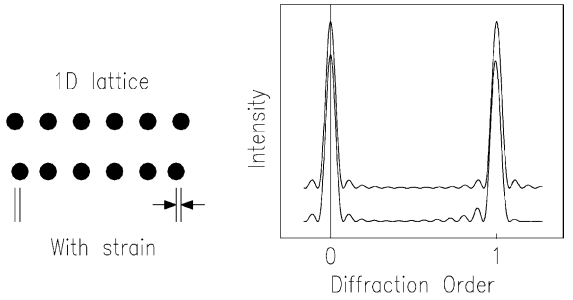

Fig. 2. Illustration of the effects of strain on the diffraction from a 1D crystal. The finite-sized array of atoms gives a diffraction pattern in the form of a slit function. When strain is introduced by displacing atoms as shown in the lower trace, the diffraction pattern becomes asymmetric around its first-order maximum.

periodic and centrosymmetric about the origin; it is therefore also symmetric about each reciprocal lattice point. When the object is strained by inward displacement of its end atoms, as shown in the lower panel, the relative weight of the diffraction features is shifted outwards, resulting in the clear breaking of the symmetry shown in the lower calculated curve.

This picture can be expressed mathematically using the usual notation of the real and reciprocal lattices. The density function $\rho(\boldsymbol{r})$ inside the finite-sized crystal can be idealized to be a set of delta functions:

$$\rho(\boldsymbol{r}) = e(\boldsymbol{r})\sum_{\boldsymbol{R}}\delta(\boldsymbol{r}-\boldsymbol{R}),$$

where the real binary-valued function $e(\boldsymbol{r})$ represents the volume in space occupied by the crystal, which we call the ''envelope function''. The infinite crystal lattice is denoted $\boldsymbol{R} = n_1\boldsymbol{a}_1 + n_2\boldsymbol{a}_2 + n_3\boldsymbol{a}_3$ spanned by the integers n_i and the lattice vectors $\boldsymbol{a}_i$. When the crystal is strained, the atoms are displaced by a vector strain field, $\boldsymbol{u}(\boldsymbol{R})$, which is itself a function of position. The density becomes

$$\rho'(\boldsymbol{r}) = e(\boldsymbol{r})\sum_{\boldsymbol{R}}\delta(\boldsymbol{r}-\boldsymbol{R}-\boldsymbol{u}(\boldsymbol{R})).$$

The reciprocal lattice, defined conventionally by the Laue equation $\boldsymbol{q}\cdot\boldsymbol{R} = 2\pi(\text{integer})$, is another lattice of points at discrete values of $\boldsymbol{q}$, $\boldsymbol{Q} = m_1\boldsymbol{b}_1 + m_2\boldsymbol{b}_2 + m_3\boldsymbol{b}_3$ spanned by the integers m_i and the reciprocal lattice vectors $\boldsymbol{b}_i$. We are interested in the effect of the strain on the diffraction near to a particular reciprocal lattice point $\boldsymbol{Q}$. We can approximate $\rho'(\boldsymbol{r})$ near to this

point by considering its Fourier transform,

$$A(\boldsymbol{q}) = \int \rho'(\boldsymbol{r})\exp(\mathrm{i}\boldsymbol{q}\boldsymbol{r})\,\mathrm{d}\boldsymbol{r} = VE(\boldsymbol{q}) * \sum_{\boldsymbol{R}}\exp(\mathrm{i}\boldsymbol{q}(\boldsymbol{R}+\boldsymbol{u}(\boldsymbol{R}))),$$

where $E(\boldsymbol{q})$ is the Fourier transform of the envelope $e(\boldsymbol{r})$ and the asterisk ($*$) denotes convolution. V is a normalization factor. In this step, we have used the convolution theorem, noting that $A(\boldsymbol{q})$ is the Fourier transform of the product of two functions. We have also employed the "picking" property of delta functions to evaluate the Fourier transform of the lattice function. When the strain is small, this summation can be approximated,

$$\sum_{\boldsymbol{R}}\exp(\mathrm{i}\boldsymbol{q}(\boldsymbol{R}+\boldsymbol{u}(\boldsymbol{R}))) \approx \sum_{\boldsymbol{R}}\exp(\mathrm{i}\boldsymbol{q}\boldsymbol{R})(1+\mathrm{i}\boldsymbol{q}\boldsymbol{u}(\boldsymbol{R})) \approx \sum_{\boldsymbol{R}}\exp(\mathrm{i}\boldsymbol{q}\boldsymbol{R})(1+\mathrm{i}\boldsymbol{Q}\boldsymbol{u}(\boldsymbol{R})).$$

The first approximation is the expansion of the exponential for small $\boldsymbol{u}$. The second approximation is valid because we are only interested in the region of reciprocal space in the immediate vicinity of $\boldsymbol{q} \approx \boldsymbol{Q}$. Once we have made the approximations, we can reverse the convolution to redefine the strained crystal density in terms of that of the unstrained crystal,

$$\rho'(\boldsymbol{r}) \approx e(\boldsymbol{r})\sum_{\boldsymbol{R}}\delta(\boldsymbol{r}-\boldsymbol{R})(1+\mathrm{i}\boldsymbol{Q}\boldsymbol{u}(\boldsymbol{R})) = e(\boldsymbol{r})\sum_{\boldsymbol{R}}\delta(\boldsymbol{r}-\boldsymbol{R})(1+\mathrm{i}\boldsymbol{Q}\boldsymbol{u}(\boldsymbol{r})) = e'(\boldsymbol{r})\sum_{\boldsymbol{R}}\delta(\boldsymbol{r}-\boldsymbol{R})$$

in terms of a *complex* envelope function, $e'(\boldsymbol{r}) = e(\boldsymbol{r})(1+\mathrm{i}\boldsymbol{Q}\boldsymbol{u}(\boldsymbol{r}))$, whose imaginary part represents the projection of the strain field $\boldsymbol{u}(\boldsymbol{r})$ onto the chosen direction $\boldsymbol{Q}$. This derivation shows that a strained crystal can be approximated by an unstrained one in which the displaced atoms are assigned densities that are complex-valued.

It is important to note that the atomic resolution is unimportant to the final result concerning the envelope, except, of course, in assuming a crystal gives rise to a periodic diffraction pattern in the first place. Strain fields inside the crystals are generally slow-varying on the atomic scale. We have demonstrated that the strain gives rise to a slow-varying imaginary part to the envelope function, which can therefore be imaged. Nanometer (i.e. sub-atomic) resolution images of the strain distribution within the crystalline grains would be extremely useful in determining the interactions between the crystal grains inside the materials.

A two-dimensional example of the diffraction from a strained object is shown in Fig. 3. At the top left is a real envelope function, $e(\boldsymbol{r})$, defining a crystal shape, which happens to be taken from a scanning-electron microscope image of a partially-annealed array of gold nanocrystals on a glass substrate. To the right is its Fourier transform, which shows the expected local symmetry. Below is a representation of a complex envelope function, $e'(\boldsymbol{r})$, where the amplitude is the same as before and the phase has been caused to vary quadratically as a function of radius from the center of the object. The shaded (colored) rings represent phase reversals. Its Fourier transform (below right) shows the diffraction expected from such a strained particle. This has clearly lost the local symmetry of the unstrained case on the left, but still resembles it in its main features, the flares and the fringes. This example shows clearly the main point of our discussion, that the *shape* of a small crystal is related to the symmetric part of its coherent diffraction pattern, while its internal *strain* appears as an asymmetry in the diffraction.

The new method we are proposing, on the basis of this discussion, is to image the strain by measuring the *asymmetric* part of the diffraction pattern surrounding some Bragg point, $\boldsymbol{q} = \boldsymbol{Q}$, using the CXD method. If this is inverted using one of the iterative methods described above, a real-space constraint must be applied in order to achieve the convergence. The simplest constraint would be to limit the spatial extent of the object by applying a boundary, usually chosen to be slightly larger than the object, this guarantees the degree of oversampling needed for the solution to be determined [7]. If an additional constraint, that the object density be real, is also applied, the resulting calculated diffraction pattern will be forced to have the local inversion symmetry about $\boldsymbol{Q}$. If, however, this requirement is relaxed, the asymmetry can be fitted and the resulting shape function will become complex; its real part will represent the physical shape of the crystal, while the imaginary part will measure directly the magnitude of the displacement field projected onto

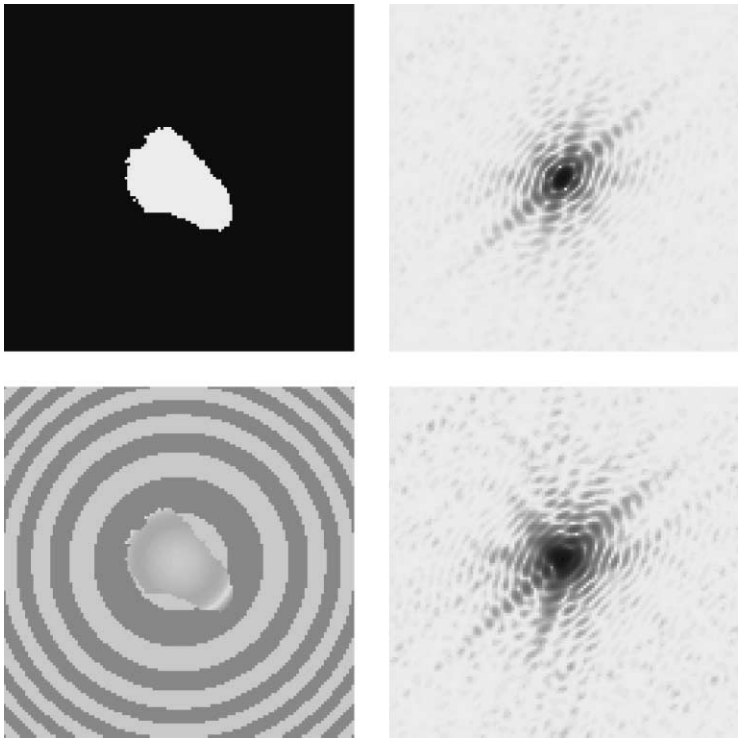

Fig. 3. Illustration of the effects of strain on the diffraction from a 2D crystal. The upper panel show an unstrained object and its calculated coherent diffraction pattern. The lower panel is the same with the addition of a real-space strain increasing quadratically with radius from the center of the object. The alternate circular shading denotes positions for which the phase lies between 0 and π or between π and 2π.

the vector $\boldsymbol{Q}$. For an unknown object, it might be envisaged that the procedure would be applied in two stages, the first to determine the shape and the second to locate the strains.

The method has already been demonstrated in one dimension, by mapping the strains present in an epitaxial thin film of Cu_3Au(1 1 1) grown on sapphire [18]. No special lengths were taken to assure the coherence of the X-ray source that was used. Nevertheless, the diffraction was coherent in 1D because a Si(1 1 1) monochromator was used and the films were only 150 Å thick. Diffraction patterns, resembling the example of Fig. 2, were measured at the (1 1 1), (2 2 0) and (3 3 1) Bragg peaks. The asymmetry became stronger from one peak to the next because of the increasing perpendicular component of the momentum transfer. The data was fit using a GS method with a fixed envelope function, $e(z)$, where z is the position within the thin film. A variable phase value was then allowed for each z. The phase function was fitted by GS separately for the profiles of the three Bragg peaks. The three curves were found to agree with each other quite well and gave the strain as a function of position. The strain led to a net outward relaxation of 0.1 Å, building up linearly over the outermost 20 Å, and was present on both sides of the film.

The general method we have described will produce a real-space map of the strain component within a nanocrystalline grain, superimposed on an image of the grain's shape (envelope). If other Bragg reflections can be measured also, other components of the strain can be determined too, eventually to build up a full strain tensor for every point inside the crystal. The spatial resolution would be determined by how far from the Bragg points the diffraction signal can be detected. Since the grains of a polycrystalline material will have different orientations, they can be imaged independently so that the strain fields on either side of

an inter-granular contact or grain boundary can be determined. We expect this method to have widespread applicability.

Acknowledgements

This work was supported by the U.S. National Science Foundation under DMR98-76610.

References

[1] I.K. Robinson, I.A. Vartanyants, M.A. Pfeifer, G.M. Williams, J.A. Pitney, accepted for publication in Phys. Rev. Lett.
[2] B.E. Warren, X-ray Diffraction, Addison Wesley, 1969.
[3] M. von Laue, Annalen der Physik 26 (1936) 55–85.
[4] I.K. Robinson, Phys. Rev. B 33 (1986) 3830.
[5] M. Tolan, S.K. Sinha, Physica B 248 (1998) 399–404.
[6] I.A. Vartanyants, I.K. Robinson, accepted for publication in J. Phys. Condensed Matter.
[7] D. Sayre, Imaging Processes and Coherence in Physics, Springer Lecture Notes in Physics 112, 1980, 229.
[8] G. Bricogne, Acta Crystallogr. A 40 (1984) 410–445.
[9] B.C. Wang, Methods Enzymol. 115 (1985) 90–112.
[10] J. Miao, P. Charalambous, J. Kirz, D. Sayre, Nature 400 (1999) 342–344.
[11] R.A. Crowther, Acta Crystallogr. B 25 (1969) 2571–2580.
[12] M.G. Rossmann, D.M. Blow, Acta Crystallogr. A 16 (1963) 39–45.
[13] R.W. Gerchberg, W.O. Saxton, Optik 35 (1972) 237.
[14] R.P. Millane, J. Opt. Soc. Am. A 7 (1990) 394–411.
[15] I.A. Vartanyants, J.A. Pitney, J.L. Libbert, I.K. Robinson, Phys. Rev. B 55 (1997) 13193–13202.
[16] I.K. Robinson, J.L. Libbert, I.A. Vartanyants, J.A. Pitney, D.M. Smilgies, D.L. Abernathy, G. Grübel, Phys. Rev. B 60 (1999) 9965–9972.
[17] R.P. Millane, W.J. Stroud, J. Opt. Soc. Am. A 14 (1997) 568–579.
[18] I. Vartanyants, C. Ern, W. Donner, H. Dosch, W. Caliebe, Appl. Phys. Lett. 77 (2000) 3929–3931.